# PREDICTING PLANETS IN *KEPLER* MULTI-PLANET SYSTEMS

Julia Fang[1] and Jean-Luc Margot[1,2]
[1] Department of Physics and Astronomy, University of California, Los Angeles, CA 90095, USA
[2] Department of Earth and Space Sciences, University of California, Los Angeles, CA 90095, USA
*Received 2011 December 1; accepted 2012 March 13; published 2012 April 30*

## ABSTRACT

We investigate whether any multi-planet systems among *Kepler* candidates (2011 February release) can harbor additional terrestrial-mass planets or smaller bodies. We apply the packed planetary systems hypothesis that suggests all planetary systems are filled to capacity, and use a Hill stability criterion to identify eight two-planet systems with significant gaps between the innermost and outermost planets. For each of these systems, we perform long-term numerical integrations of $10^7$ years to investigate the stability of 4000–8000 test particles injected into the gaps. We map out stability regions in orbital parameter space, and therefore quantify the ranges of semimajor axes and eccentricities of stable particles. Strong mean-motion resonances can add additional regions of stability in otherwise unstable parameter space. We derive simple expressions for the extent of the stability regions, which is related to quantities such as the dynamical spacing $\Delta$, the separation between two planets in units of their mutual Hill radii. Our results suggest that planets with separation $\Delta < 10$ are unlikely to host extensive stability regions, and that about 95 out of a total of 115 two-planet systems in the *Kepler* sample may have sizeable stability regions. We predict that *Kepler* candidate systems including KOI 433, KOI 72/Kepler-10, KOI 555, KOI 1596, KOI 904, KOI 223, KOI 1590, and KOI 139 can harbor additional planets or low-mass bodies between the inner and outer detected planets. These predicted planets may be detected by future observations.

*Key words:* methods: numerical – planetary systems – planets and satellites: dynamical evolution and stability – stars: individual (KOI 433, KOI 72/Kepler-10, KOI 555, KOI 1596, KOI 904, KOI 223, KOI 1590, KOI 139)

*Online-only material:* color figures

## 1. INTRODUCTION

Early studies of extrasolar planetary systems showed residual velocity trends in Keplerian orbit fits to radial velocity data (e.g., Marcy & Butler 1998; Butler et al. 1998; Marcy et al. 1999; Vogt et al. 2000; Fischer et al. 2001), suggesting that these systems may host additional, undetected planets. Fischer et al. (2001) noted that about half of the stars in their sample of 12 systems showed residual trends greater than the expected scatter due to measurement uncertainties and stellar noise. Most of these systems were later confirmed to harbor additional planet(s).

In more recent years, the study and prediction of undiscovered planets have been aided by long-term *N*-body simulations. These numerical investigations searched for stability zones in multi-planet systems by integrating hundreds to thousands of test bodies, which were injected into empty regions between known planets (e.g., Menou & Tabachnik 2003; Barnes & Raymond 2004; Raymond & Barnes 2005; Ji et al. 2005; Rivera & Haghighipour 2007; Raymond et al. 2008). For example, a putative Saturn-mass planet in HD 74156 was first predicted by Raymond & Barnes (2005) through numerical simulations that showed a stable region between planets b and c. The planet was later discovered by Bean et al. (2008), although there have been questions about the validity of the detection (Wittenmyer et al. 2009; Meschiari et al. 2011). This prediction was motivated by the packed planetary systems (PPS) hypothesis.

The PPS hypothesis is the idea that planetary systems are formed dynamically full and filled to capacity, and any additional planets will cause the systems to be unstable (e.g., Barnes & Raymond 2004; Raymond & Barnes 2005; Raymond et al. 2006; Barnes & Greenberg 2007). Consequently, planetary systems with stable stability zones between the innermost and outermost planets are suggestive of additional, yet-undetected planets. Reasons for the non-detections of hypothetical planets

include lack of sufficient data, such as non-transiting planets that require more data to detect them via transit timing variations, or planetary masses/radii that are below detection limits. The orbital properties of predicted planets can be identified through long-term numerical simulations. Support for the PPS hypothesis comes from early observations of packed multi-planet systems that led to this hypothesis (e.g., Butler et al. 1999; Marcy et al. 2001a, 2001b; Fischer et al. 2002; Mayor et al. 2004), apparent consistency between the planet–planet scattering model and packed systems (Raymond et al. 2009), the remarkably dense and packed Kepler-11 system (Lissauer et al. 2011a), theoretical work (e.g., Chambers et al. 1996; Smith & Lissauer 2009), and other investigations (e.g., Rivera & Lissauer 2000; Goździewski & Migaszewski 2006).

In the present study, we apply the PPS hypothesis to multi-planet candidate systems discovered by the *Kepler* team during the mission's first four and a half months of data (Borucki et al. 2011). The *Kepler* mission is a transit survey designed to search for Earth-sized planets (Borucki et al. 2010; Koch et al. 2010; Jenkins et al. 2010; Caldwell et al. 2010) and is sensitive to terrestrial-class and larger planets located at a large range of separations from their host star. *Kepler* can detect multiple transiting systems for densely packed planets with nearly coplanar configurations or with serendipitous geometric alignment, and the dynamics and statistics of *Kepler* multi-planet systems are providing a wealth of information about planetary systems (e.g., Steffen et al. 2010; Latham et al. 2011; Lissauer et al. 2011a, 2011b).

Given that planetary systems have been discovered with densely packed planets, we seek to test the PPS hypothesis and predict additional planets in *Kepler* candidate multi-planet systems. In Section 2, we discuss *Kepler*'s sample of multi-planet systems as well as our methodology for evaluating each planetary system's level of dynamical packing. We also explain

our methods for running numerical simulations and our choice of initial conditions. In Section 3, we present the results from long-term numerical integrations and illustrate them using stability maps. Section 4 discusses the dynamical interpretation of our work, in particular the relationship between planetary spacing and the extent of an inter-planet stability region. We then summarize the restrictions and scope of our study (Section 5) and state our conclusions (Section 6).

## 2. DATA AND METHODS

Based on publicly available *Kepler* data covering the first four and a half months of observations, about one-third of ∼1200 transiting planet candidates are hosted in multi-planet systems (Borucki et al. 2011; Lissauer et al. 2011b). These multi-planet systems include 115 systems with 2 transiting planets, 45 systems with 3 transiting planets, 8 systems with 4 transiting planets, 1 system with 5 transiting planets, and 1 system with 6 transiting planets. Most *Kepler* candidate planets have not been validated and are therefore Kepler Objects of Interest (KOI) and assigned a number. Candidates in multi-planet systems have a smaller probability than single-planet candidates of being an astrophysical false positive (Ragozzine & Holman 2010; Latham et al. 2011; Lissauer et al. 2011a, 2012). Moreover, all of these candidate multi-planet systems are stable over long-term integrations (Lissauer et al. 2011b). For the remainder of this paper, we refer to all candidate planets and systems by dropping the adjective "candidate." All of these *Kepler* multi-planet systems presented by Borucki et al. (2011) are examined using the analytical method described below in Section 2.1.

To discern the extent of packing in *Kepler* multi-planet systems, we define two types of stability as outlined by Gladman (1993). Fulfillment or overfulfillment of these stability criteria, meaning that the considered planetary system is not on the verge of instability, can imply the presence of additional planets according to the PPS hypothesis. First, Hill stability requires that a system's ordering of planets (in terms of distance from the star) remains constant. This means that close approaches are forbidden and planet crossing is not allowed for all time, but the outer planet may be unbound and still be Hill stable. The second type of stability is Lagrange stability, which is a stricter definition than Hill stability. Lagrange stability requires not only the conservation of the ordering of planets, but also that they remain bound to the star for all time. Hill stability can be mathematically examined for two-planet, non-resonant systems, and Lagrange stability is typically examined through numerical simulations. Hill stability can be a reasonable predictor of Lagrange stability (Barnes & Greenberg 2006). In the next two subsections, we examine Hill stability through analytical methods (Section 2.1) and Lagrange stability through *N*-body integrations (Section 2.2) for *Kepler* multi-planet systems.

### 2.1. Analytical Method

We calculate the Hill stability criterion of each adjacent planet pair in *Kepler* multi-planet systems. We follow the notation given in Barnes & Greenberg (2006) by referring to the relevant quantities as $\beta$ and $\beta_{\rm crit}$:

$$\beta = \frac{-2(M_* + M_1 + M_2)}{G^2(M_1 M_2 + M_* M_1 + M_* M_2)^3} L^2 E \qquad (1)$$

$$\beta_{\rm crit} = 1 + 3^{4/3} \frac{M_1 M_2}{M_*^{2/3}(M_1 + M_2)^{4/3}} - \frac{M_1 M_2 (11 M_1 + 7 M_2)}{3 M_* (M_1 + M_2)^2} + \cdots, \qquad (2)$$

where $M_*$ is the mass of the star, $M_1$ and $M_2$ are the masses of the planets where $M_1 > M_2$, $L$ and $E$ are the total orbital angular momentum and energy of the system, and $G$ is the gravitational constant (Marchal & Bozis 1982; Gladman 1993; Veras & Armitage 2004). Two-planet, non-resonant systems with $\beta/\beta_{\rm crit} \geqslant 1$ are considered Hill stable. For systems with additional planets and/or in resonance, stability needs to be investigated numerically. A system that does not fulfill the Hill stability criterion has unknown Hill stability; it may or may not be Hill stable. In Equations (1) and (2), $\beta_{\rm crit}$ is only a function of masses and $\beta$ is a function of masses as well as semimajor axes and eccentricities; evidently, for a given set of masses, there are stability boundaries in orbital parameter space.

We calculate $\beta/\beta_{\rm crit}$ for each adjacent planet pair in *Kepler* multi-planet systems released as of 2011 February by Borucki et al. (2011). We find that almost all of the adjacent planet pairs have $\beta/\beta_{\rm crit}$ values greater than 1. Raymond et al. (2009) discussed that planet pairs with values of $\beta/\beta_{\rm crit}$ greater than ∼1.5–2 are probably capable of harboring additional planet(s) with a semimajor axis in between those of the existing planets. We find eight *Kepler* systems, all of which are two-planet systems, with $\beta/\beta_{\rm crit}$ values of 1.5 or greater (Table 1). None of the three-planet, four-planet, five-planet, and six-planet systems have any adjacent planet pairs with $\beta/\beta_{\rm crit}$ values of at least 1.5. In the next section, we place test particles in each of these eight systems to determine their zones of stability.

Another useful criterion for evaluating stability is the dynamical spacing $\Delta$ between two planets, i.e., the difference between their semimajor axes expressed in units of their mutual Hill radius,

$$\Delta = \frac{a_2 - a_1}{R_{H1,2}}, \qquad (3)$$

where $R_{H1,2}$ is the mutual Hill radius defined as

$$R_{H1,2} = \left(\frac{M_1 + M_2}{3 M_*}\right)^{1/3} \frac{a_1 + a_2}{2}, \qquad (4)$$

(e.g., Gladman 1993; Chambers et al. 1996). Here, subscripts 1 and 2 denote the inner and outer planets, respectively.

### 2.2. Numerical Method

The previous section identified eight *Kepler* systems with $\beta/\beta_{\rm crit} > 1.5$ (Table 1), which suggests that these systems are most likely to have gaps between adjacent planets that may contain additional planet(s). For these eight systems, we numerically explore their regions of Lagrange stability to determine zones in orbital element space that can harbor additional, undetected planets that are stable. We use a hybrid symplectic/Bulirsch–Stoer algorithm from an *N*-body integration package, Mercury (Chambers 1999), with a time step that sampled 1/20th of the innermost planet's orbit.

For each of the eight identified *Kepler* systems, our simulations include the star and its two detected planets as well as 4000–8000 massless[3] test particles placed in between the locations of the inner and outer planets. We do not assign a common

---

[3] It would be ideal to perform detailed integrations of numerous test bodies with non-zero masses, distributed with varying distances and velocities from the star to sample all possible orbits. However, this process would be very computationally costly. Since we are investigating the stability of terrestrial-mass planets or smaller bodies, we approximate such objects as massless test particles in our simulations. These test particle approximations have been similarly adopted in previous studies (i.e., Rivera & Haghighipour 2007 and references therein).

**Table 1**
Identified *Kepler* Systems with $\beta/\beta_{\rm crit} > 1.5$

| KOI | $M_*$ ($M_\odot$) | $M_1$ ($M_\oplus$) | $R_1$ ($R_\oplus$) | $a_1$ (AU) | $P_1$ (days) | $M_2$ ($M_\oplus$) | $R_2$ ($R_\oplus$) | $a_2$ (AU) | $P_2$ (days) | $\beta/\beta_{\rm crit}$ | $\Delta$ |
|---|---|---|---|---|---|---|---|---|---|---|---|
| 433 | 1.01 | 37.38 | 5.80 | 0.050 | 4.030 | 209.81 | 13.40 | 0.935 | 328.240 | 2.861 | 28.7 |
| 72[a] | 1.03 | 1.72 | 1.30 | 0.018 | 0.837 | 5.56 | 2.30 | 0.252 | 45.295 | 2.781 | 90.3 |
| 555 | 0.95 | 2.31 | 1.50 | 0.046 | 3.702 | 5.56 | 2.30 | 0.376 | 86.496 | 2.031 | 77.3 |
| 1596 | 0.87 | 5.56 | 2.30 | 0.061 | 5.924 | 13.21 | 3.50 | 0.416 | 105.355 | 1.817 | 53.4 |
| 904 | 0.69 | 4.61 | 2.10 | 0.029 | 2.211 | 9.61 | 3.00 | 0.159 | 27.939 | 1.624 | 50.4 |
| 223 | 0.92 | 7.74 | 2.70 | 0.041 | 3.177 | 6.07 | 2.40 | 0.226 | 41.008 | 1.621 | 56.2 |
| 1590 | 0.88 | 3.75 | 1.90 | 0.033 | 2.356 | 8.34 | 2.80 | 0.163 | 25.780 | 1.527 | 55.4 |
| 139 | 1.07 | 1.46 | 1.20 | 0.045 | 3.342 | 36.07 | 5.70 | 0.741 | 224.794 | 1.508 | 54.1 |

**Notes.** Eight *Kepler* multi-planet systems are identified with $\beta/\beta_{\rm crit}$ values greater than 1.5. We list their KOI identifier, stellar mass $M_*$, planetary masses $M_1$ and $M_2$, planetary radii $R_1$ and $R_2$, semimajor axes $a_1$ and $a_2$, orbital periods $P_1$ and $P_2$, $\beta/\beta_{\rm crit}$ value (listed in descending order), and dynamical spacing criterion $\Delta$. The inner planet has the subscript 1 and the outer planet has the subscript 2. Stellar mass and planetary parameters (size, semi-major axis, and period) are taken from Borucki et al. (2011), and we derived the planetary masses using a power law: $M_i = (R_i/R_\oplus)^{2.06} M_\oplus$ where the subscript $i$ represents planet 1 or 2 (Lissauer et al. 2011b). [a] KOI 72 is a confirmed system and is also known as Kepler-10 (Batalha et al. 2011).

number of test particles to each system for computational cost reasons. The overall cost of the integration is a function of the time step and of the number of test particles. Systems that have inner planets with shorter orbital periods (and therefore shorter time steps) are assigned fewer test particles so that the integrations may finish within a reasonable amount of time. In total, we integrate $\sim$8000 test particles per system except for KOI 72 ($\sim$4000 test particles) and KOI 904 ($\sim$6000 test particles). Each system is integrated for $10^7$ years, and test particles that survive the length of the integration are considered stable test particles.

For each of the eight identified *Kepler* systems, initial conditions for the star and its two detected planets are given in Table 1. These initial conditions include the star's mass and the known planets' masses, radii, semimajor axes, and orbital periods. The other orbital elements of the planets—eccentricity, inclination, argument of pericenter, longitude of the ascending node, and mean anomaly—are currently unknown; we assume circular and coplanar orbits and assign a random mean anomaly for the planets. The coplanar assumption is supported by the fact that these are all transiting planets; the larger the mutual inclination between the planets' orbital planes, the smaller the probability that they all transit the star (Ragozzine & Holman 2010). Circular and coplanar orbits have the least angular momentum deficit and therefore are most likely to be stable configurations (Laskar 1997).

Initial conditions for test particles are as follows. Inclinations $i$ are drawn from a uniform distribution ($0° < i < 5°$). Previous work by Lissauer et al. (2011b) initially suggested that *Kepler* multi-planet systems have low relative inclinations with a mean of $\lesssim5°$, but that number was revised to $\lesssim10°$ as our paper was undergoing revisions. Semimajor axis $a$ and eccentricity $e$ are initially drawn from a uniform distribution ($a_1 < a < a_2$; $0 < e < 1$) for the first 1000 particles for each system. Subsequent integrations of additional test particles were randomly inserted into semimajor axis and eccentricity bins that had few or no particles, by filling up bins with lower eccentricity first. This ensured better coverage of semimajor axis and eccentricity space. All other orbital elements (argument of pericenter, longitude of the ascending node, and mean anomaly) are drawn randomly from a uniform distribution between $0°$ and $360°$.

This procedure is performed for each of the eight *Kepler* systems identified with $\beta/\beta_{\rm crit} > 1.5$ (shown in Table 1). For each system, we record each test particle's starting orbital elements and whether it became unstable or remained stable

during the duration of the integration. Instability can be due to ejection or collision of the test particle with another body.

## 3. RESULTS

In this section, we describe the results stemming from long-term *N*-body integrations of eight *Kepler* systems (Table 1). All of these multi-planet systems have two known planets and were identified in Section 2.1 as potentially capable of containing an additional planet in the regions between the inner and outer planets. For each of these systems, we quantify their zones of stability and instability in semimajor axis and eccentricity space by illustrating them in stability maps plotted in Figures 1 and 2.

Our stability maps and results indicate that each of these planetary systems are capable of harboring a stable low-mass body for up to $10^7$ years in the intermediate zone between the known inner and outer planets. We discover broad stable regions in each planetary system, which appear as mountain-shaped regions in Figures 1 and 2. We also find additional regions of stability outside the mountain regions, where test particles can have stable orbits due to mean-motion resonances with the inner and outer planets. Strong first-order resonances with the outer planet are marked in Figures 1 and 2. As for instabilities, the majority (typically $\sim$90%) of unstable test particles were unstable within the first $10^6$ years.

Stable test particles do not show much movement in semimajor axis and eccentricity over the course of an integration. As a result, the plots shown in Figures 1 and 2 only show the starting locations of test particles. We quantify the motion of test particles in orbital element space by computing the median of the absolute values of the differences between initial and final values of semimajor axis and eccentricity. The median semimajor axis differences range from $\sim3.8 \times 10^{-6}$ AU to $\sim2.3 \times 10^{-4}$ AU, and the median eccentricity differences range from $\sim2.4 \times 10^{-4}$ to $\sim8.5 \times 10^{-4}$. The largest differences in semimajor axis and eccentricity for stable particles are commonly due to particles placed near the edge of the stability region that became scattered off to another part of the stability region, or particles originally not in the stability region that became scattered to an orbit with a final semimajor axis greater than the outer planet's semimajor axis and typically accompanied by an increase in eccentricity.

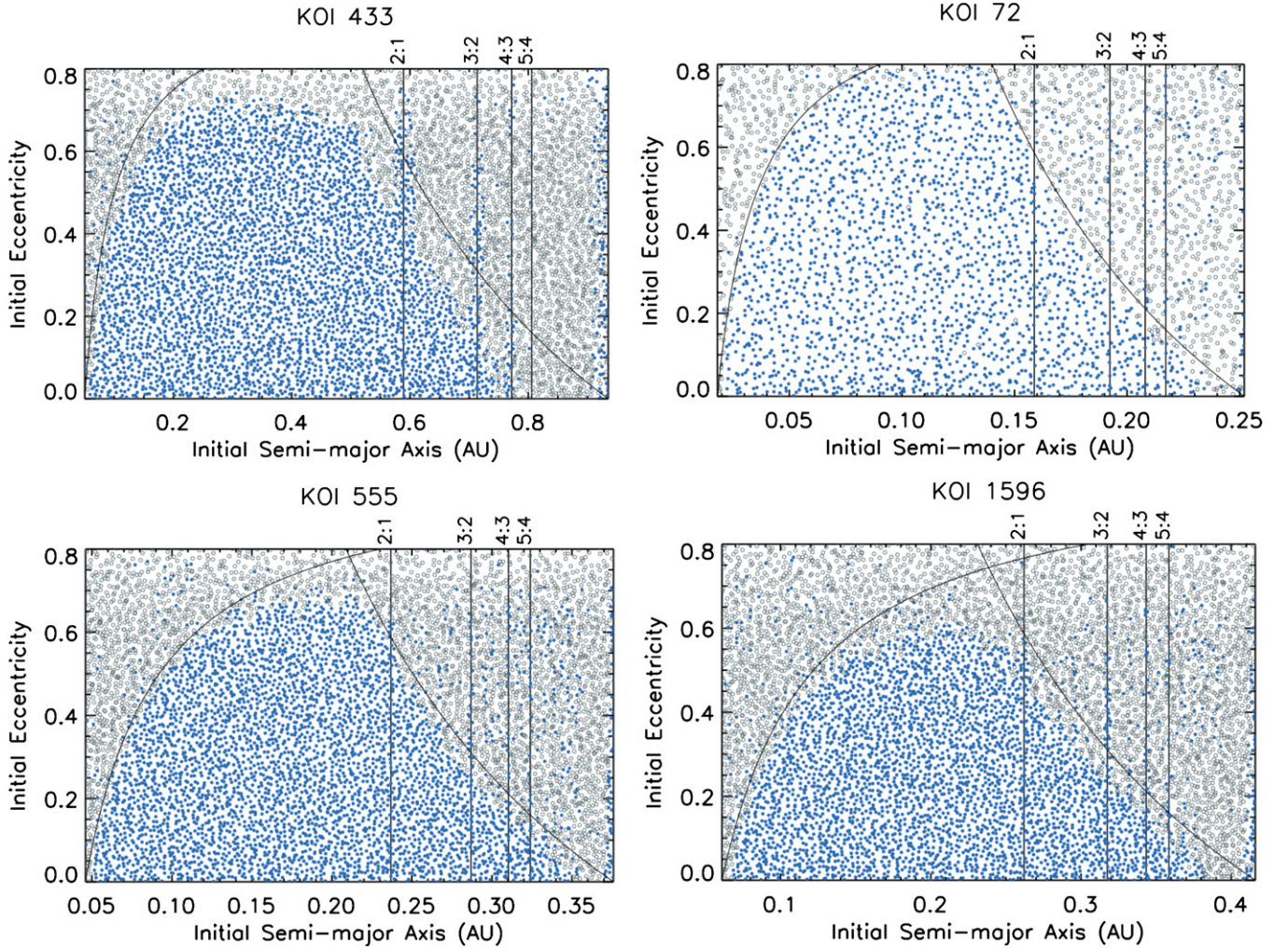Mean motion resonances can act as additional reservoirs of stability outside of the mountain-shaped region. Strong

**Figure 1.** Stability maps for KOI 433, KOI 72/Kepler-10, KOI 555, and KOI 1596. Test particles, shown as circles, are displayed at their starting values of semimajor axis and eccentricity. Filled blue circles are test particles that survived the integration length of $10^7$ years, and unfilled gray circles are test particles that did not remain stable in that time. Black curves show the boundaries dividing planet crossing and non-planet crossing orbits. Vertical black lines represent the locations of first-order mean-motion resonances with the outer planet. The inner and outer planets are located at the left and right edges of the plot, respectively.

(A color version of this figure is available in the online journal.)

first-order resonances are plotted in Figures 1 and 2 to provide examples of stable test particles in resonances outside of the stability region. Many more first-order and higher-order resonances exist, forming a thicket of resonance locations that are not drawn to reduce confusion. We find that the majority of stable test particles outside the mountain are located in resonant or near-resonant periods with that of the inner or outer planet. Test particles placed in planet-crossing orbits (above the black curves drawn in Figures 1 and 2) can be stable if placed in such resonances, which protect the test particles from close encounters with the planets. The role of mean motion resonances in the stability of test particles and planets has also been previously explored (e.g., see Rivera & Haghighipour 2007; Barnes & Greenberg 2007).

Our results show that massless test particles can stably orbit in these stability regions for up to $10^7$ years, and we suggest that these stability results can be extended from massless particles to Earth-mass planets. Spot checks performed for KOI 1596, which has a moderate (for this sample) $\beta/\beta_{\rm crit}$ of $\sim$1.817, indicate that an Earth-mass planet with a semimajor axis in the middle of the stability region and with an eccentricity of zero is stable for at least $10^7$ years. We have also tested scenarios where we

increased the mass of the inserted planet up to a few Earth masses, as well as cases where we inserted two, three, and four evenly spaced, Earth-mass planets with zero eccentricities in the main stability region. These integrations all proved to be stable for up to $10^7$ years in our tests for KOI 1596. As a result, it is likely that the stability zones identified using massless test particles are applicable to Earth-mass bodies, and that these stability zones can potentially contain more than one Earth-mass planet.

We briefly compare our numerical results with analytical expectations. Our stability results based on this sample of *Kepler* systems indicate that two-planet systems meeting the analytical threshold $\beta/\beta_{\rm crit} > 1.5$ are consistent with the idea that they can hold additional planet(s) in intermediate separations from their host star. All eight systems investigated here had planet pairs with $\beta/\beta_{\rm crit} > 1.5$ and were numerically found to be unpacked, which supports previous work suggesting that additional planets are expected to be stable in systems with $\beta/\beta_{\rm crit} > 1.5$–2 (Raymond et al. 2009). Since all eight *Kepler* systems we investigated with $\beta/\beta_{\rm crit} > 1.5$ are unpacked, we expect that there may also be additional systems with $\beta/\beta_{\rm crit}$ less than 1.5 that are also unpacked (see the next section).
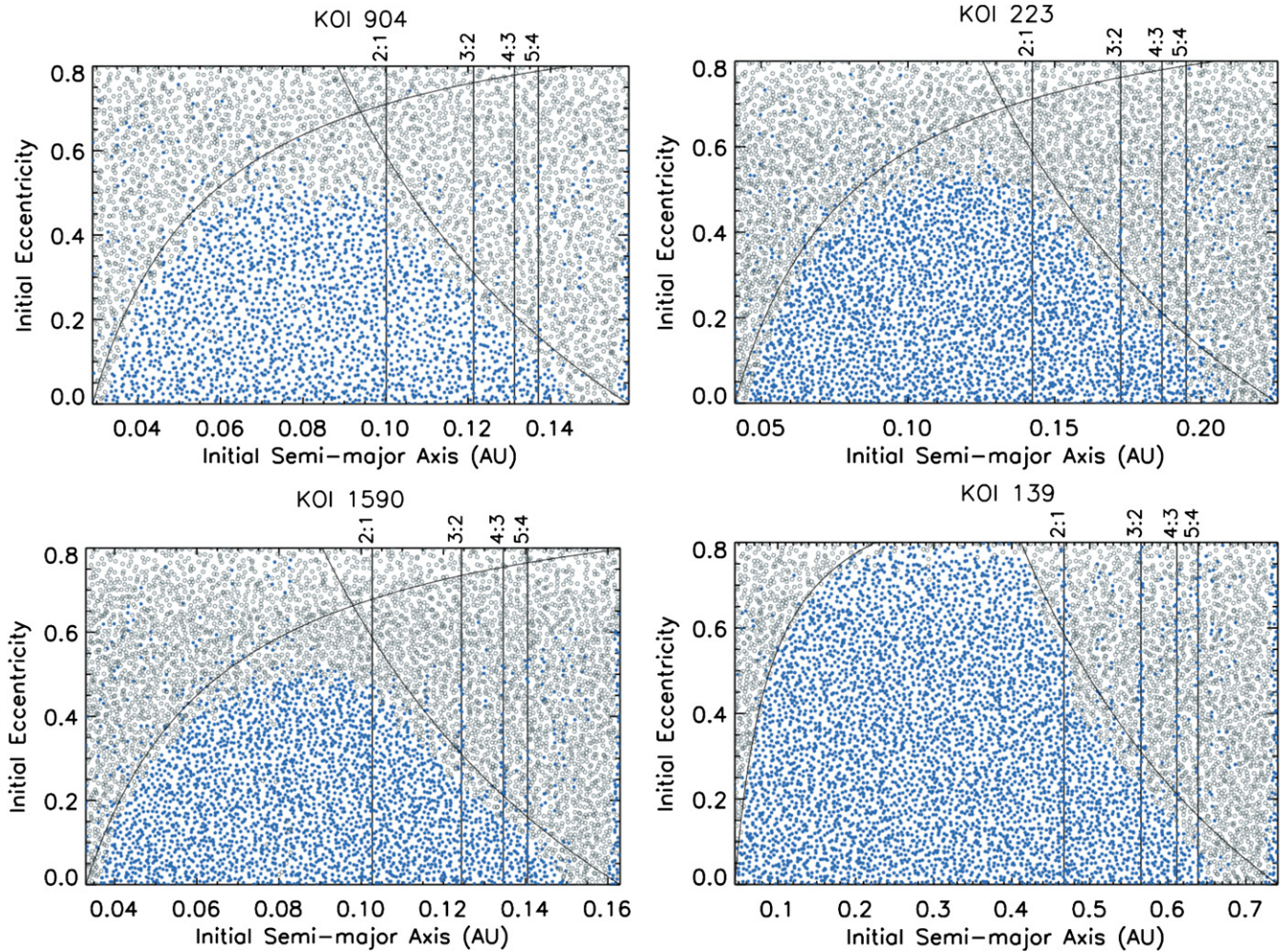
**Figure 2.** Same as Figure 1, except we show stability plots for KOI 904, KOI 223, KOI 1590, and KOI 139.
(A color version of this figure is available in the online journal.)

## 4. PLANETARY SPACING DETERMINES EXTENT OF STABILITY REGION

We now describe in greater detail the shapes and sizes of the mountain-shaped stability regions observed in Figures 1 and 2. In particular, we discuss the relationships between the spacing between two planets and the extent of the stability region in between the planets.

The stable regions in each planetary system include a mountain-shaped stability peninsula as well as narrow strips of stability due to mean-motion resonances (e.g., see Figures 1 and 2). The large mountain-shaped stability region has a shape common to all of the planetary systems because it is sculpted on the left and right flanks by specific semimajor axis and eccentricity values that delineate planet-crossing orbits. Mathematically, the mountain's left slope is shaped by $a_1 = a(1 - e)$, where $a_1$ is the inner planet's semimajor axis. The mountain's right slope is shaped by $a_2 = a(1 + e)$, where $a_2$ represents the outer planet's semimajor axis. These orbit-crossing boundaries are shown as black curves in each stability plot in Figures 1 and 2. The actual stability boundaries (left and right flanks of the mountain-shaped stability region) do not extend all the way to the black curves. This is explained by close approach effects: test particles that are not initially on planet-crossing orbits can become unstable if they make sufficiently close approaches to the existing planets. The critical distance from the planet-crossing boundary at

which this can occur is similar to the half-width of a planet's feeding zone in which planetesimals may impact the planet, which can be estimated at about $\sim$2.3 Hill radii for circular orbits (i.e., Greenberg et al. 1991). The results of our simulations show similar distances between the planet-crossing curve and the actual slope of the mountain.

The maximum height of each mountain-shaped stability region is constrained by the semimajor axes of the inner and outer planets. The maximum eccentricity allowed is determined by the intersection of the orbit-crossing boundaries, $a_1 = a(1 - e)$ and $a_2 = a(1 + e)$, and serves as an upper limit to the maximum possible height of the stability mountain. Since we assume that the two known planets in each system have orbital eccentricities of zero, the intersection of the curves occurs at a semimajor axis of $(a_1 + a_2)/2$ and an eccentricity of

$$e_{\max} = 1 - \frac{2a_1}{a_1 + a_2}, \quad (5)$$

which is the maximum possible eccentricity $e_{\max}$ of the stability mountain. As is evident in Figures 1 and 2, the actual peak of the stability region is not the same as the $e_{\max}$.

The actual height or peak of each mountain-shaped stability region can be computed as follows. Consider a test particle located between the inner and outer planets. In order to remain stable, this particle cannot enter a zone of dynamical
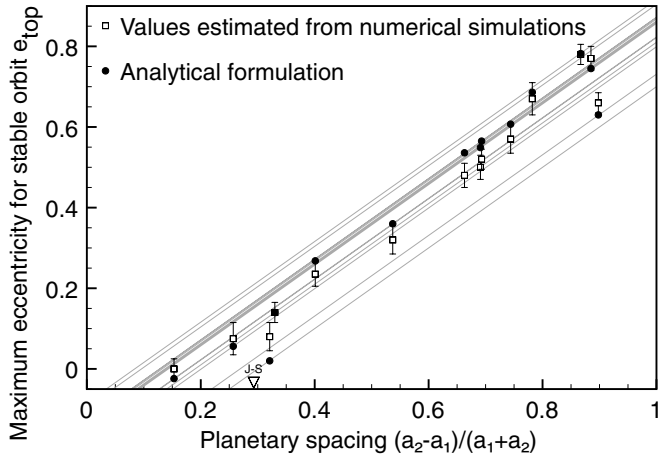
**Figure 3.** Maximum eccentricity for a stable test particle orbit at a semimajor axis $(a_1 + a_2)/2$ between two existing planets. The unfilled squares represent estimates of $e_{top}$ with their uncertainties, and the filled circles and gray lines represent values of $e_{top}$ computed from Equation (10) for various planetary systems (eight systems listed in Table 1 plus six additional systems for a larger sample). For comparison, the inverted triangle shows the planetary spacing between Jupiter and Saturn (note that we only considered two-planet systems with circular orbits, and our results may not be applicable to systems with greater multiplicity of planets or non-circular orbits).

influence surrounding each planet. We measure this exclusion zone as a certain number $c_i$ of Hill radii $R_{Hi}$, where $R_{Hi} = (M_i/(3M_*))^{1/3}a_i$ and the subscript $i = 1, 2$ refers to the inner and outer planets, respectively. Therefore, a stable test particle's pericenter $q = a(1 - e)$ and apocenter $Q = a(1 + e)$ distances must obey

$$q = a(1 - e) > a_1 + c_1 R_{H1} \tag{6}$$

$$Q = a(1 + e) < a_2 - c_2 R_{H2}, \tag{7}$$

where the inner and outer planets are assumed to have circular orbits. We label the maximum stable eccentricity as $e_{top}$ (flat top of the mountain) and consider the midpoint between the two planets $(a_1 + a_2)/2$. We can rewrite Equations (6) and (7) for particles on the edge of stability/instability as

$$\frac{(a_1 + a_2)}{2}(1 - e_{top}) = a_1 + c_1 R_{H1} \tag{8}$$

$$\frac{(a_1 + a_2)}{2}(1 + e_{top}) = a_2 - c_2 R_{H2}. \tag{9}$$

If we subtract the two equations from each other and solve for $e_{top}$, we obtain

$$\begin{aligned} e_{top} &= \frac{a_2 - a_1 - c_1 R_{H1} - c_2 R_{H2}}{a_1 + a_2} \\ &= -\frac{c_1 R_{H1} + c_2 R_{H2}}{a_1 + a_2} + \frac{a_2 - a_1}{a_1 + a_2}. \end{aligned} \tag{10}$$

We empirically determine $c_1$ and $c_2$ by fitting Equation (10) in a least-squares sense to values of $e_{top}$ measured from Figures 1 and 2. We find $c_1 = 19.733$ and $c_2 = 4.1877$. Comparison between computed values of $e_{top}$ (using Equation (10)) and the measured values of $e_{top}$ (from Figures 1 and 2) is shown in Figure 3, which illustrates the maximum stable eccentricity $e_{top}$ as a function of planetary spacing for a range of planetary masses.

The width of a stability mountain's base (where $e = 0$) can be related to the dynamical spacing criterion $\Delta$ between two
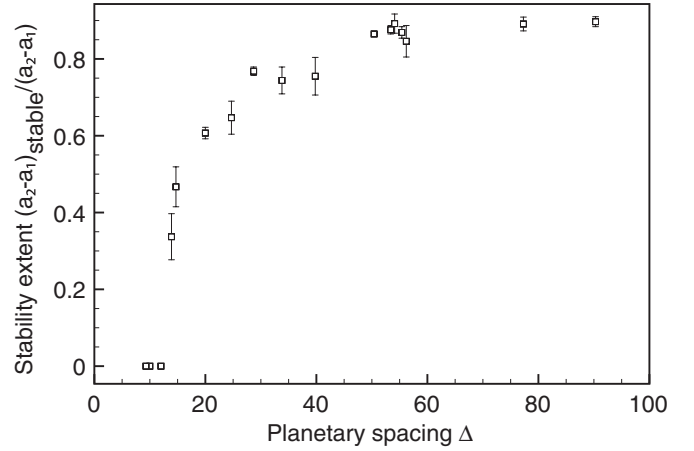


**Figure 4.** Fraction of planetary separation $(a_2 - a_1)$ with stable test particles at $e = 0$, as a function of planetary spacing criterion $\Delta$. The unfilled squares represent the results from numerical simulations in this study (eight planetary systems from Table 1 plus nine additional systems for a larger sample) with error bars representing measurement uncertainties.

planets (see Equations (3) and (4)). A system with two planets in a circular and coplanar state satisfies Hill stability (orbits do not cross) if $\Delta$ is greater than $2\sqrt{3}$, or $\sim 3.46$ (Gladman 1993). The stability of systems with more than two planets is less well characterized and is commonly determined using numerical calculations. Estimates of the width $(a_2 - a_1)_{stable}$ of each stability mountain's base at $e = 0$ (ignoring the effects of resonances as much as possible) are related to $\Delta$ (Figure 4). We do not find any stability regions for planetary systems with $\Delta \lesssim 10$.

We generalize the results shown in Figure 4 to a broader context. From this figure, we can determine a critical value of $\Delta$ that divides two-planet systems with stable versus no stable regions. This crossover occurs in the range $\Delta_{crit} = 10$–15. Accordingly, we suggest that two-planet systems similar to those explored in this paper cannot have extensive stability zones if their separations have $\Delta$ less than 10. Similarly, we predict that stable regions can exist in systems with $\Delta$ greater than 15. In the 2011 February *Kepler* release (Borucki et al. 2011; Lissauer et al. 2011b), 95 out of a total of 115 two-planet systems have $\Delta > 15$, or 82.6% of all two-planet systems in this sample can potentially harbor stability zones within the known planets. The results discussed here and illustrated in Figure 4 are consistent with previous studies. Chambers et al. (1996) numerically studied coplanar and circular configurations of 3, 5, 10, and 20 planet systems, and found no stable systems with planetary spacing of $\Delta < 10$. More recently, Smith & Lissauer (2009) examined the packing density of systems with three, five, and nine Earth-mass planets in circular and coplanar orbits with planets equally spaced in terms of $\Delta$. They conducted long-term numerical integrations up to 10 billion years, and demonstrated that three-planet systems are stable when the spacing between neighboring planets is roughly $\Delta \sim 7$. Other previous results on spacing between planets or protoplanets include the typical $\sim 10$ Hill radii spacing between neighboring protoplanets, as seen in simulations of protoplanetary accretion from a swarm of planetesimals (Kokubo & Ida 1998, 2000, 2002).

## 5. SCOPE AND LIMITATIONS OF OUR RESULTS

Given the large amount of possible parameter space that can be explored in stability studies, we summarize the limitations

and scope of results stemming from this paper. We also discuss any other assumptions and considerations that may change our results.

*Sample.* We solely investigated multi-planet systems announced by the *Kepler* team in the 2011 February release of candidate systems (Borucki et al. 2011). No other planetary systems were considered. Therefore, our sample has the same biases as any *Kepler* detection, including the observational preference toward short-period planets given the transit detection method. Our study is also limited to *Kepler* systems for which there are two known planets, and we do not investigate the dynamical spacing in systems with greater multiplicity of planets.

*Masses.* The planetary masses are typically not known for these KOI systems. We estimated masses using *Kepler*-measured planetary sizes with a power law (Table 1, Lissauer et al. 2011b) obtained from fitting to Earth and Saturn. However, the densities and true masses of *Kepler* planets can be different from these assumptions, which could change our results.

*Eccentricities.* Eccentricity is another important dynamical parameter that is not known for most *Kepler* multi-planet systems. We have assumed zero eccentricities for the known planets in our numerical calculations, and this assumption is consistent with the expected tidal circularization of close-in planets. For the only confirmed planetary system in our sample, KOI 72 or Kepler-10, photometry and radial velocity data suggest that Kepler-10b has zero eccentricity (Batalha et al. 2011). Non-zero eccentricities of the planets in our sample, if present, would change the locations of stability regions of test particles.

*Inclinations.* We assumed zero inclinations between the orbits of known planets in our sample as well as low inclinations up to $\sim 5°$ for test particles. Consequently, our results can only be applied to systems that are relatively coplanar. The assumption of coplanarity or near-coplanarity is reasonable for multi-planet systems discovered by the transit technique at the heart of the *Kepler* mission, given that the inclination dispersion of these systems appears to have mean of $\lesssim 10°$.

*Integration time.* We integrated test particles for a time span of $10^7$ years due to CPU time limitations, but more accurate modeling can be obtained by using a longer integration time period. There may be test particles that are stable over $10^7$ years but not over longer timescales, although our simulations show that $\sim 90\%$ of particles unstable in $10^7$ years were unstable within the first $10^6$ years.

## 6. CONCLUSION

The PPS model is based on the idea that all planetary systems are formed to capacity. To test this hypothesis, we investigated the packing density of *Kepler* candidate two-planet systems from the first four and a half months of the mission. Through numerical calculations, we determined whether regions of stability exist between known planets with wide separations, i.e., in systems that seemed the most unpacked based on how well they satisfy Hill stability. Discovery of a stable region suggests that a low-mass body could be present in the gap, which would then bring the system to a more packed state. With time, such predictions will be shown to be correct or incorrect, allowing us to gauge the success of this model.

We performed detailed numerical simulations of eight two-planet *Kepler* systems, selected using an analytical $\beta/\beta_{\mathrm{crit}}$ stability criterion. In addition to the known planets, we included 4000–8000 test particles per planetary system, allowing both circular and non-circular, and coplanar and non-coplanar orbits.

These test particles are good proxies for low-mass bodies such as terrestrial planets as well as small bodies such as asteroids or dwarf planets. We integrated all bodies for $10^7$ years; we defined stable particles as those that remained stable during the length of the integration and unstable particles as particles that experienced a collision or ejection.

Our results (Figures 1 and 2) indicated that all of the planetary systems investigated here (KOIs 433, 72, 555, 1596, 904, 223, 1590, and 139) can pack additional, yet-undetected bodies in the identified stable locations. We also discussed relationships relating dynamical spacing between known planets and the extent of the inter-planet stability region. We derived an analytical relationship relating the largest possible eccentricity of a stable test particle to the semimajor axes and Hill radii of the two planets surrounding the particle. We also demonstrated that $\Delta$, the separation between two planets in units of their mutual Hill radii, can be a reasonable predictor of whether or not stability regions can exist between planets. The cutoff occurs at a critical $\Delta$ between 10 and 15. We suggest that planets with separation $\Delta < 10$ are unlikely to host extensive stability regions. Based on this $\Delta = 10$–15 cutoff, we suggest that about 95 out of a total of 115 two-planet systems in the 2011 February *Kepler* sample may have sizeable stability regions.

We thank the referee for useful comments.

*Note added in proof.* After submission of this paper, Batalha et al. (2012) released an updated catalog of transiting planet candidates. One of the systems studied in this paper, KOI 904, was found to have three additional planets, two of which are in our predicted stability zone.

## REFERENCES

Barnes, R., & Greenberg, R. 2006, ApJ, 647, L163
Barnes, R., & Greenberg, R. 2007, ApJ, 665, L67
Barnes, R., & Raymond, S. N. 2004, ApJ, 617, 569
Batalha, N. M., Borucki, W. J., Bryson, S. T., et al. 2011, ApJ, 729, 27
Batalha, N. M., Rowe, J. F., Bryson, S. T., et al. 2012, arXiv:1202.5852
Bean, J. L., McArthur, B. E., Benedict, G. F., & Armstrong, A. 2008, ApJ, 672, 1202
Borucki, W. J., Koch, D., Basri, G., et al. 2010, Science, 327, 977
Borucki, W. J., Koch, D. G., Basri, G., et al. 2011, ApJ, 736, 19
Butler, R. P., Marcy, G. W., Fischer, D. A., et al. 1999, ApJ, 526, 916
Butler, R. P., Marcy, G. W., Vogt, S. S., & Apps, K. 1998, PASP, 110, 1389
Caldwell, D. A., Kolodziejczak, J. J., Van Cleve, J. E., et al. 2010, ApJ, 713, L92
Chambers, J. E. 1999, MNRAS, 304, 793
Chambers, J. E., Wetherill, G. W., & Boss, A. P. 1996, Icarus, 119, 261
Fischer, D. A., Marcy, G. W., Butler, R. P., Laughlin, G., & Vogt, S. S. 2002, ApJ, 564, 1028
Fischer, D. A., Marcy, G. W., Butler, R. P., et al. 2001, ApJ, 551, 1107
Gladman, B. 1993, Icarus, 106, 247
Goździewski, K., & Migaszewski, C. 2006, A&A, 449, 1219
Greenberg, R., Bottke, W. F., Carusi, A., & Valsecchi, G. B. 1991, Icarus, 94, 98
Jenkins, J. M., Caldwell, D. A., Chandrasekaran, H., et al. 2010, ApJ, 713, L87
Ji, J., Liu, L., Kinoshita, H., & Li, G. 2005, ApJ, 631, 1191
Koch, D. G., Borucki, W. J., Basri, G., et al. 2010, ApJ, 713, L79
Kokubo, E., & Ida, S. 1998, Icarus, 131, 171
Kokubo, E., & Ida, S. 2000, Icarus, 143, 15
Kokubo, E., & Ida, S. 2002, ApJ, 581, 666
Laskar, J. 1997, A&A, 317, L75
Latham, D. W., Rowe, J. F., Quinn, S. N., et al. 2011, ApJ, 732, L24
Lissauer, J. J., Fabrycky, D. C., Ford, E. B., et al. 2011a, Nature, 470, 53
Lissauer, J. J., Marcy, G. W., Rowe, J. F., et al. 2012, arXiv:1201.5424
Lissauer, J. J., Ragozzine, D., Fabrycky, D. C., et al. 2011b, ApJS, 197, 8
Marchal, C., & Bozis, G. 1982, Celest. Mech., 26, 311
Marcy, G. W., & Butler, R. P. 1998, ARA&A, 36, 57
Marcy, G. W., Butler, R. P., Fischer, D., et al. 2001a, ApJ, 556, 296

Marcy, G. W., Butler, R. P., Vogt, S. S., Fischer, D., & Liu, M. C. 1999, ApJ, 520, 239
Marcy, G. W., Butler, R. P., Vogt, S. S., et al. 2001b, ApJ, 555, 418
Mayor, M., Udry, S., Naef, D., et al. 2004, A&A, 415, 391
Menou, K., & Tabachnik, S. 2003, ApJ, 583, 473
Meschiari, S., Laughlin, G., Vogt, S. S., et al. 2011, ApJ, 727, 117
Ragozzine, D., & Holman, M. J. 2010, arXiv:1006.3727
Raymond, S. N., & Barnes, R. 2005, ApJ, 619, 549
Raymond, S. N., Barnes, R., & Gorelick, N. 2008, ApJ, 689, 478
Raymond, S. N., Barnes, R., & Kaib, N. A. 2006, ApJ, 644, 1223

Raymond, S. N., Barnes, R., Veras, D., et al. 2009, ApJ, 696, L98
Rivera, E., & Haghighipour, N. 2007, MNRAS, 374, 599
Rivera, E. J., & Lissauer, J. J. 2000, ApJ, 530, 454
Smith, A. W., & Lissauer, J. J. 2009, Icarus, 201, 381
Steffen, J. H., Batalha, N. M., Borucki, W. J., et al. 2010, ApJ, 725, 1226
Veras, D., & Armitage, P. J. 2004, Icarus, 172, 349
Vogt, S. S., Marcy, G. W., Butler, R. P., & Apps, K. 2000, ApJ, 536, 902
Wittenmyer, R. A., Endl, M., Cochran, W. D., Levison, H. F., & Henry, G. W. 2009, ApJS, 182, 97